Combination between [B-α-SiW_9O_{34}] unit and triangular inorganic Ni_6 core under hydrothermal conditions: from monomer to rare dimer with malposed dodeca-Nickel centers

Lei Yang[a,b], *Yu Huo*[a] *and Jingyang Niu* [a]*

[a] *Institute of Molecular and Crystal Engineering, College of Chemistry and Chemical Engineering, Henan University, Kaifeng, Henan 475004 P. R. China*
[b] *The department of physics-chemistry, Henan Polytechnic University, Jiaozuo, Henan 454150 P. R. China*

Supporting Information

This file includes:

Section S1. Experimental Section

Inductively coupled plasma (ICP) spectra were performed on a Perkin–Elmer Optima 3300DV ICP instrument. Analyses for H were carried out on a Perkin-Elmer 240C elemental analyzer. IR spectra were obtained from a solid sample palletized with KBr on Nicolet 170 SXFT-IR spectrometer in the range 400-4000 cm^{-1}. Thermogravimetric analyses were performed in N_2 on a Perkin-Elmer-7 instrument with a heating rate of 10 °C/min. XRPD measurements were performed on a Philips X'Pert-MPD instrument with CuKα radiation (λ = 1.54056A) at 293 K. Magnetic susceptibility measurements were obtained by the use of a Quantum Design MPMS-XL7 SQUID magnetometer at a temperature ranging from 2 to 300 K.

Synthesis considerations:

1. **1** and **2** can also be successfully isolated when $K_4SiW_{12}O_{40}$ was replaced by $H_4SiW_{12}O_{40}$, while $K_4SiW_{12}O_{40}$ was replaced by $K_8SiW_{11}O_{39}$ or $K_{10}SiW_9O_{34}$, only tetra-Ni-sandwiched polyoxoanions $[Ni_4(H_2O)_2(B\text{-}\alpha\text{-}SiW_9O_{34})_2]^{10-}$[1] was obtained. Besides, the pretreatment of α-$K_4SiW_{12}O_{40}$ is necessary for the produce.
2. The molar ratio of Ni ions/ $K_4SiW_{12}O_{40}$ significantly influences the nuclear number of Ni clusters and the structural diversity of products; that is, the formations of tetra- or hexa-Ni clusters are mainly controlled by the molar ratio of reactants. Tetra-Ni and hexa-Ni cluster can be obtained when the molar ratio of Ni ions/ $K_4SiW_{12}O_{40}$ lie in the range of 1 − 5 and 6.66 − 20, respectively.
3. Pyridine-2,5-carboxylic acid did not exist in the final structure. However, if pyridine-2,5-carboxylic acid was not introduced into the reaction mixture, no crystal products were isolated under similar reaction conditions. So it may be presumed that pyridine-2,5-carboxylic acid might be beneficial for obtaining the high quality crystals and enhancing the product yields.
4. Under similar conditions, we expected that using other TM (Zn. Mn, Cu, Co) ions in place of Ni ions would lead to an isostructural species to **1**. Unfortunately, tetra-M-sandwiched polyoxoanions $[M_4(H_2O)_2(B\text{-}\alpha\text{-}SiW_9O_{34})_2]^{10-}$ (M = Zn. Mn, Cu, Co)[1] were obtained instead of silicotungstate containing triangular inorganic TM_6 cluster.
5. The crystals suit for X-ray crystallography can not be obtained shorter than 7 days.

1. W. H. Knoth, P. J. Domaille, R. L. Harlow, *Inorg. Chem.*, 1986, **25,** 1577.

Section S2. Tables

Table S1 Crystal data and structure refinement parameters for **1** and **2**

Empirical formula	$H_{76}Na_2Ni_{12}O_{109}Si_2W_{18}$	$H_{42}Ni_6SiW_9O_{56}$
Formula weight	5936.59	2973.34
Temperature (K)	296(2)	296(2)
Wavelength (Å)	0.71073	0.71073
Crystal system, space group	Monoclinic, *P*2(1)/*c*	orthorhombic, *Pnma*
a (Å)	16.7174(17)	18.8278 (15)
b (Å)	18.2134(19)	20.7853 (16)
c (Å)	15.0644(16)	12.2101 (10)
β / °	96.022(2)	90.00
V (Å3)	4561.5(8)	4778.3(7)
Z	2	4
Dc / g cm–3	4.291	4.133
Crystal size	0.22 × 0.15 × 0.13 mm	0.29 × 0.25 × 0.20 mm
Absorption coefficient (mm–1)	25.170	24.023
F(000)	5332	5352
Theta range for data collection (˚)	1.22 to 25.00 deg	1.93 to 28.32 deg.
Limiting indices	$-18 \leq h \leq 19$	$-24 \leq h \leq 24$
	$-21 \leq k \leq 16$	$-23 \leq k \leq 37$
	$-13 \leq l \leq 17$	$-16 \leq l \leq 13$
Reflections collected/unique	23614 / 8017 [R(int) = 0.0585]	30182 / 6061 [R(int) = 0.0884]
Data / restraints / parameters	8017 / 66 / 668	6061 / 0 / 355
Goodness-of-fit on F2	1.047	1.026
Final R indices [I>2σ(I)]	R1 = 0.0349, wR2 = 0.0786	R1 = 0.0424, wR2 = 0.1106
R indices (all data)	R1 = 0.0500, wR2 = 0.0837	R1 = 0.0816, wR2 = 0.1399

$R_1 = \sum||F_o| - |F_c||/\sum|F_o|$; $wR_2 = \{\sum[w(F_o^2-F_c^2)^2]/\sum[w(F_o^2)^2]\}^{1/2}$

Table S2 Bond-valence sum calculations[2] for **1**

W1	5.993096	W2	6.148346	W3	6.167336
W4	6.043845	W5	6.174601	W6	6.126355
W7	6.255019	W8	6.174233	W9	6.198115
Si1	3.8551N25	Ni1	2.027952	Ni2	1.947028
Ni3	1.978338	Ni4	1.972158	Ni5	2.020157
Ni6	1.972738	O1	1.925478	O2	1.676128
O3	1.990036	O4	1.727174	O5	1.699851
O6	1.752566	O7	1.77593	O8	1.753988
O9	1.990829	O10	2.020263	O11	2.000329
O12	1.934267	O13	1.953348	O14	1.988997
O15	1.709526	O16	1.963176	O17	1.871961
O18	1.932023	O19	2.019896	O20	1.912004
O21	1.923524	O22	1.87011	O23	2.082257
O24	2.044237	O25	1.832757	O26	2.030531
O27	1.912226	O28	1.85962	O29	2.015199
O30	1.992326	O31	1.861721	O32	1.88652
O33	1.857003	O34	1.935076	O35	0.329292
O36	0.329381	O37	1.1636	O38	1.125752
O39	0.312049	O40	0.328936	O41	0.339412
O42	0.344495	O43	0.33813	O44	0.305127
O45	0.335944	O46	1.101445		

Table S3 Bond-valence sum calculations for **2**

W1	6.185881	W3	6.209987	W5	6.291524
W7	6.146117	W9	6.285245	Ni1	1.956686
Ni2	2.005984	Ni3	2.032559	Ni4	1.837866
Si1	3.927126	O1	1.893777	O3	1.891115
O4	1.110051	O5	2.026554	O6	1.953745
O7	1.948816	O8	1.159256	O10	2.013492
O12	2.066812	O13	1.936176	O15	2.019009
O16	2.007523	O17	1.65945	O19	1.966766
O21	1.813276	O22	1.886804	O25	1.860514
O26	1.955108	O27	1.736066	O29	1.687492
O30	1.887146	O34	0.310871	O35	1.813766
O38	0.328226	O39	0.311796	O42	0.293797
O44	0.300381	O45	0.333862	O46	0.327694

The protonated polyoxotungstate fragment of **2** is reasonable. The reasons are as follows:

(1) The polyoxotungstate fragment has high negative charges and rich basic surface oxygen atoms, which can easily been protonated.

(2) On the basis of valence sum (∑s) calculation, the oxidation states of O atoms in **2** can be divided into five groups according to their bond valence sums. ∑s in the range of -0.35–0.0, -1.11–-1.16, -2.06–-1.9, -1.9 – -1.7, -1.7 – -1.6. So the protons are likely to be delocalized on these O atoms.

(3) In generally, the protons can not be located in polyoxometalate fragments by X-ray diffraction. They are usually assigned to be delocalized on the whole polyoxoanion only for the charge balance of the polyoxoanion. The phenomenon is common in POM chemistry and has been reported in many literatures. For example, $[H_3W_{12}O_{40}]^{5-}$,[3] $[H_{12}V_{13}O_{40}]^{3-}$,[4] $[HW_9O_{33}Ru^{II}_2(dmso)_6]^{7-}$,[5] $[Ni(enMe)_2]_3[H_6Ni_{20}P_4W_{34}(OH)_4O_{136}(enMe)_8(H_2O)_6]\cdot 12H_2O$[6] and $[Ni(en)_2(H_2O)]_2[H_8Ni_{20}P_4W_{34}(OH)_4O_{136}(en)_9(H_2O)_4]\cdot 16H_2O$.[6]

2. I. D. Brown, D. Altermatt, *Acta Crystallogr.*, Sect. 1985, **B41,** 244.

3. C.Streb, C. Ritchie, D. L. Long, P. Kögerler, L. Cronin, *Angew. Chem. Int. Ed*., 2007, **46,** 7579.

4. L. Pettersson, I. Andersson, *Inorg. Chem*., 1992, **31,** 4032.

5. L. Bi, F. Hussain, U. Kortz, M. Sadakane, M. H. Dickman, *Chem. Commun*., 2004, 1420.

6 S. T. Zheng, J. Zhang, J. M. Juan, D. Q. Yuan, G. Y. Yang, *Angew. Chem. Int. Ed*., 2009, **48,** 7176.

Table S4 Ni–O distances and Ni–O–Ni bond angles in **1**

Ni5—O34—Ni4	92.3(3)	Ni4—O9—Ni1	93.3(3)
Ni5—O34—Ni2	94.0(3)	Ni2—O10—Ni1	95.1(3)
Ni4—O34—Ni2	94.4(3)	Ni4—O14—Ni6	95.3(3)
Ni1—O37—Ni2	99.5(3)	Ni5—O13—Ni6	95.6(3)
Ni1—O37—Ni4	98.4(3)	Ni2—O11—Ni3	94.3(3)
Ni2—O37—Ni4	100.6(3)	Ni3—O12—Ni5	94.9(3)
Ni3—O38—Ni2	99.9(3)	Ni6—O46—Ni4	100.9(3)
Ni3—O38—Ni5	97.5(3)	Ni6—O46—Ni5	99.4(3)
Ni2—O38—Ni5	98.3(3)	Ni4—O46—Ni5	95.4(3)
Ni1—O37	1.982(7)	Ni2—O38	2.006(7)
Ni1—O3^i	2.056(8)	Ni2—O37	2.007(7)
Ni1—O36	2.065(9)	Ni2—O10	2.041(7)
Ni1—O35	2.065(8)	Ni2—O11	2.056(7)
Ni1—O10	2.083(7)	Ni2—O34	2.119(8)
Ni1—O9	2.093(8)	Ni2—O18^i	2.244(8)
Ni3—O38	2.001(8)	Ni4—O37	2.026(8)
Ni3—O1^i	2.055(8)	Ni4—O46	2.034(7)
Ni3—O12	2.065(8)	Ni4—O41	2.053(8)
Ni3—O40	2.065(9)	Ni4—O9	2.078(7)
Ni3—O39	2.085(9)	Ni4—O14	2.102(8)
Ni3—O11	2.126(7)	Ni4—O34	2.109(8)
Ni5—O46	2.039(8)	Ni6—O46	2.002(8)
Ni5—O38	2.044(8)	Ni6—O43	2.056(8)
Ni5—O42	2.049(8)	Ni6—O45	2.057(8)

Ni5—O12	2.066(8)	Ni6—O13	2.086(7)
Ni5—O34	2.069(7)	Ni6—O44	2.094(8)
Ni5—O13	2.075(8)	Ni6—O14	2.109(8)
O1—Ni3$^{\mathrm{i}}$	2.055(8)	O18—Ni2$^{\mathrm{i}}$	2.244(8)
O3—Ni1$^{\mathrm{i}}$	2.056(8)		

Symmetry transformations used to generate equivalent atoms: (i) x, y, z; (ii) -x, y+1/2, -z+1/2; (iii) -x, -y, -z; (iv) x, -y-1/2, z-1/2.

Table S5 Ni–O distances and Ni–O–Ni bond angles in **2**

Ni1—O8	1.993(8)	Ni2—O8$^{\mathrm{i}}$	2.015(8)
Ni1—O45	2.059(9)	Ni2—O8	2.015(8)
Ni1—O38	2.066(10)	Ni2—O10$^{\mathrm{i}}$	2.081(8)
Ni1—O46	2.068(9)	Ni2—O10	2.081(8)
Ni1—O16$^{\mathrm{i}}$	2.122(8)	Ni2—O7	2.088(11)
Ni1—O10	2.119(9)	Ni2—O34	2.086(11)
Ni3—O4	2.020(8)	Ni4—O4	2.025(11)
Ni3—O8$^{\mathrm{i}}$	2.010(8)	Ni4—O44	2.098(14)
Ni3—O16	2.064(8)	Ni4—O42$^{\mathrm{i}}$	2.107(10)
Ni3—O6	2.058(8)	Ni4—O42	2.107(10)
Ni3—O39	2.084(9)	Ni4—O6	2.109(8)
Ni3—O7	2.099(7)	Ni4—O6$^{\mathrm{i}}$	2.109(8)
O4—Ni3$^{\mathrm{i}}$	2.020(8)	O8—Ni3$^{\mathrm{i}}$	2.010(8)
O7—Ni3$^{\mathrm{i}}$	2.099(7)	O16—Ni1$^{\mathrm{i}}$	2.122(8)
Ni2—O7—Ni3$^{\mathrm{i}}$	93.9(4)	Ni3—O4—Ni3$^{\mathrm{i}}$	97.8(5)
Ni3—O7—Ni3$^{\mathrm{i}}$	93.0(4)	Ni3—O4—Ni4	99.5(4)
Ni1—O8—Ni2	99.5(4)	Ni3$^{\mathrm{i}}$—O4—Ni4	99.5(4)
Ni1—O8—Ni3$^{\mathrm{i}}$	101.0(3)	Ni3—O6—Ni4	95.7(3)
Ni2—O8—Ni3$^{\mathrm{i}}$	99.0(3)	Ni2—O7—Ni3	93.9(4)
Ni3—O16—Ni1$^{\mathrm{i}}$	95.1(3)	Ni2—O10—Ni1	93.5(3)

Symmetry transformations used to generate equivalent atoms: (i) x, y, z; (ii) -x+1/2, -y, z+1/2; (iii) x+1/2, -y+1/2, -z+1/2; (iv) -x, y+1/2, -z; (v) -x, -y, -z; (vi) x-1/2, y, -z-1/2; (vii) -x-1/2, y-1/2, z-1/2; (viii) x, -y-1/2, z

Section S3.Additional Structural Figures

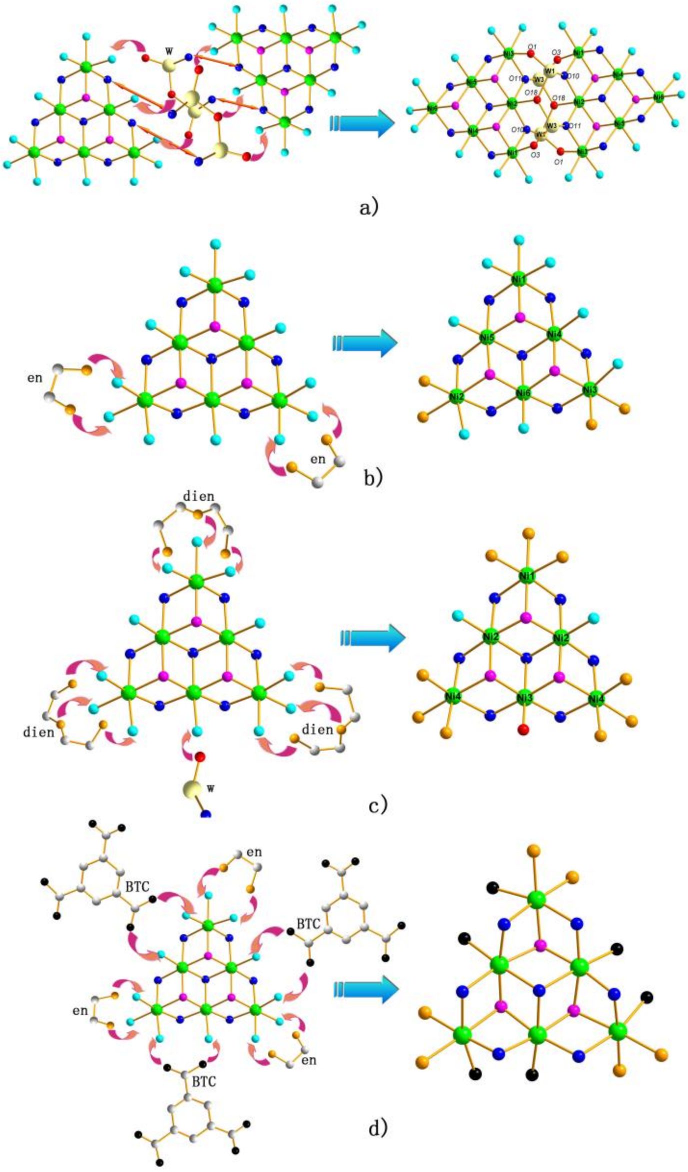

Fig.S1 The ball-and-stick representation of {Ni_6} in compounds: a) Double inorganic {Ni_6} in **1** combined by four W atoms *via* ten bridge O atoms, remaining 18 terminal water ligands. It can be described as that three terminal water ligands of one edge in $Ni_6(OH)_3(H_2O)_{12}$ are replaced by three O atoms from WO_6 of SiW9B unit; b) Hybrid {Ni_6} in $[\{Ni_6(\mu_3\text{-}OH)_3(en)_2(H_2O)_8\}(B\text{-}\alpha\text{-}PW_9O_{34})]\cdot 7H_2O$ [12] remaining 8 terminal water ligands, C atoms omitted for clarity. It can be described as that four water ligands of vertex in $Ni_6(OH)_3(H_2O)_{12}$ are replaced by four N atoms from two en ligands; c) Hybrid {Ni_6} in $[Ni_6(\mu_3\text{-}OH)_3(H_2O)_2(dien)_3(B\text{-}\alpha\text{-}PW_9O_{34})]]\cdot 4H_2O$[11] , remaining 2 terminal water ligands. Nine terminal water ligands of vertex in $Ni_6(OH)_3(H_2O)_{12}$ are replaced by nine N atoms from three dien ligands and one middle water ligands is replaced by one O atom from WO_6 of SiW9B unit; d) Hybrid Ni_6-cluster in $[Ni(en)_2(H_2O)_2]_6\{Ni_6(Tris)(en)_3(BTC)_{1.5}(B\text{-}\alpha\text{-}PW_9O_{34})_8\cdot 12en\cdot 54H_2O$ (en = ethylenediamine, BTC =1,3,5-benzenetricarboxylate). [13c] All the terminal water ligands of $Ni_6(OH)_3(H_2O)_{12}$ are replaced by six N atoms from three en molecules and six O atoms from three BTC ligands. (Color code: Ni, green; W, yellow; O atoms from hydroxy, purple; O atoms from XW_9A unit, blue; O from XW_9B unit, red; O atoms from terminal water, sky blue; O atoms from organic ligands, black; N, orange; C, grey)

In the inorganic {Ni_6} of **1:** Ni3 and Ni1 ions are combined with two O atoms from SiW9A fragment, one O atom from SiW9B unit, one O atom from hydroxy and two terminal water ligands; Ni4 and Ni5 ions are bonded to six oxygen atoms, three O atoms from SiW9A fragment, two O atoms from hydroxyls and one O atom from terminal water ligand; Ni2 ion is coordinated by three O atoms from SiW9A fragment, one O atom from SiW9B unit and two O atom from hydroxyls; Ni6 ion is linked to two O atoms from SiW9A fragment, one O atom from hydroxy and three terminal water ligands.

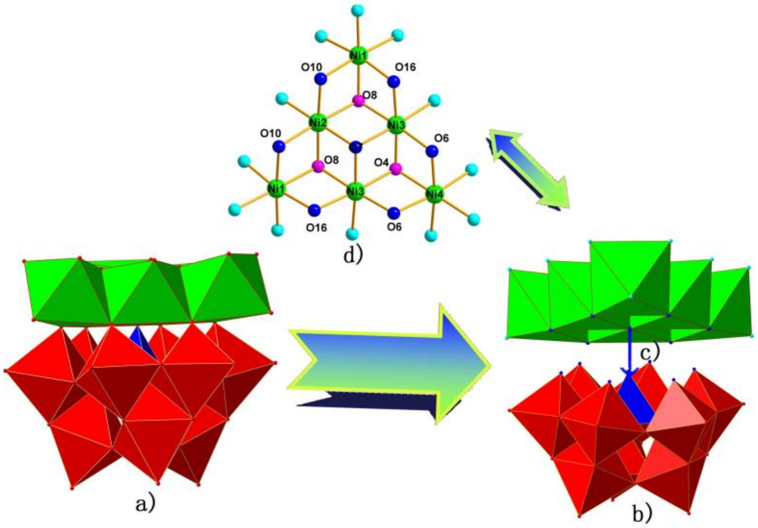

Fig.S2 (a) Side view of **2**, water molecules omitted for clarity; (b) View of B-α-$[SiW_9O_{34}]^{10-}$ unit; (c) Polyhedral representation of $\{Ni_6\}$; (d) Ball-stick representation of $\{Ni_6\}$. The distances for W–O and Ni–O: 1.697(8)–2.388(10) A˚ and 1.993(8)–2.122(8) A˚, respectively. (Color code: WO_6, red; SiO_4, blue; NiO_6, green; O atoms from SiW_9, blue; O atoms from terminal water, sky blue; O atoms from hydroxyls, purple)

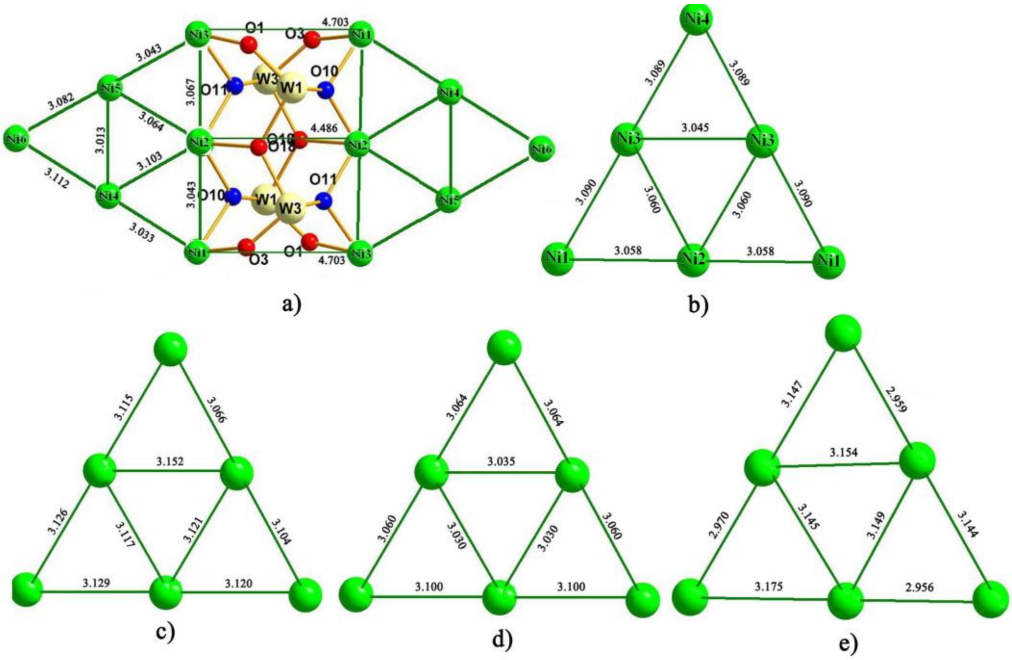

Fig. S3. Schematic of $\{Ni_6\}$ incarnating Ni…Ni distances in: (a) **1**; (b) **2**; (c) $[\{Ni_6(\mu_3\text{-}OH)_3(en)_2(H_2O)_8\}(B\text{-}\alpha\text{-}PW_9O_{34})]\cdot 7H_2O$;[12] (d) $[Ni_6(\mu_3\text{-}OH)_3(H_2O)_2(dien)_3(B\text{-}\alpha\text{-}PW_9O_{34})]\cdot 4H_2O$;[11] (e) $[Ni(en)_2(H_2O)_2]_6\{Ni_6(Tris)(en)_3(BTC)_{1.5}(B\text{-}\alpha\text{-}PW_9O_{34})_8\cdot 12en\cdot 54H_2O$.[13c]

Section S4. Additional $1/\chi_M$ –T, TGA, IR and PXRD

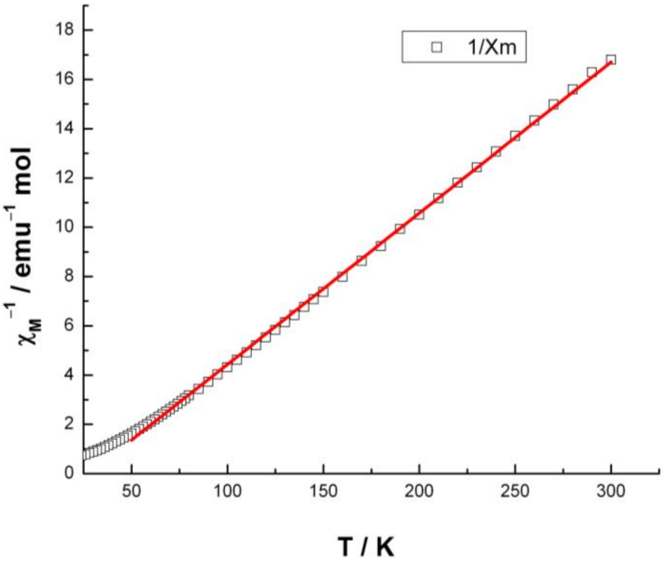

Fig.S4 The temperature dependence of $1/\chi_M$ and the linear fit of the temperature dependence $1/\chi_M$ in the range of 50–300 K for **1**,

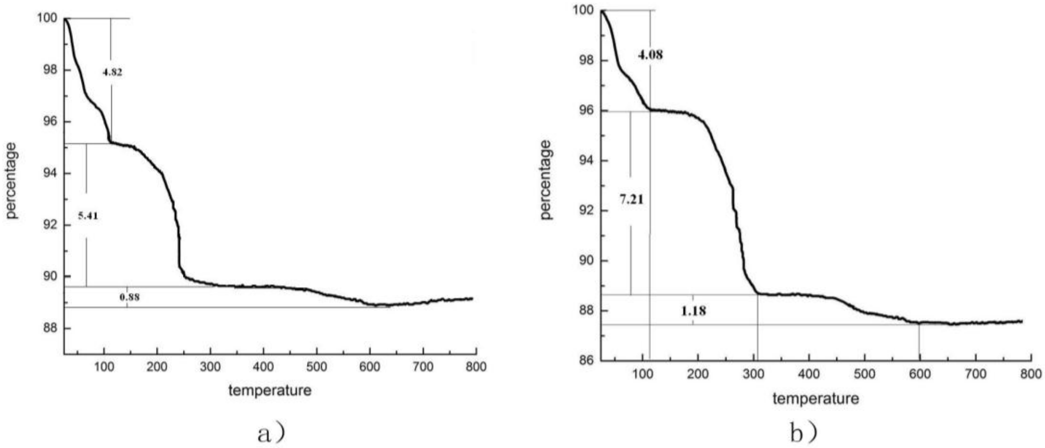

Fig.S5 TG curves a) for **1** b) for **2**

The TG curves of **1** and **2** show three step weight loss processes in the range of 30–800 ºC. The first weight loss 4.82 (calcd 5.15%) for **1** and 4.08 (calcd 4.24 %) for **2** occurred in the range 30-110 ºC is assigned to the release of 17 crystal water molecules for **1** (7 crystal water molecules for **2**). The second weight loss 5.44 (calcd 5.46%) for **1** and 7.21 (calcd 7.26 %) for **2** occurred in the range 110-300 ºC belongs to 18 and 12 coordinated water molecules respectively, following weight loss 0.88 (calcd 0.91%) for **1** and 1.18 (calcd 1.21%) for **2** in the range of 300–600ºC is corresponded to the removal of 3 and 2 structure water molecules respectively. The total weight loss of **1** is 11.14 % (calcd 11.52%) and total weight loss of **2** is 12.47 % (calcd 12.71 %).

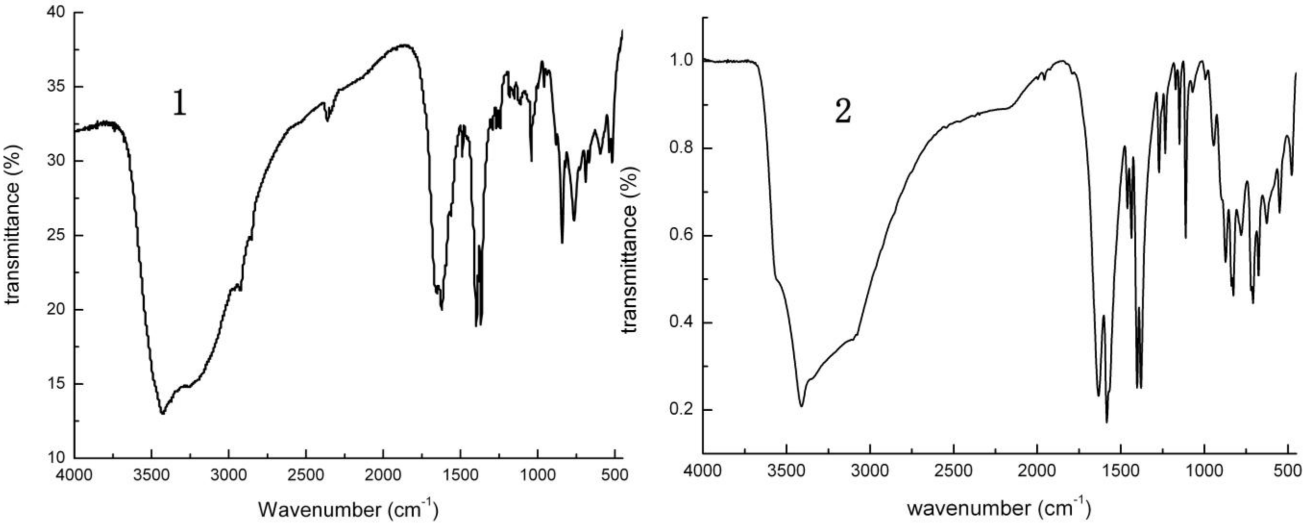

Fig.S6 IR spectra of **1** and **2**

The IR spectra of **1** and **2** show the characteristic vibration patterns resulting from Keggin POM framework in the range of 1100–700 cm^{-1}. Four groups of characteristic vibration absorption bands resulting from Keggin-type silicotungstate framework are observed at 1053, 948, 898–777 and 707 cm^{-1} in **1** and 1040, 956, 878–766, 727 in **2**, which are attributed to the stretching vibration of ν(Si–O), ν(W=O$_t$), ν(W–O$_b$) and ν(W–O$_c$), respectively. Bands in the 400-764 cm^{-1} region are characteristics of v (M-O-M) (M = W or Ni) and v (Ni-O).

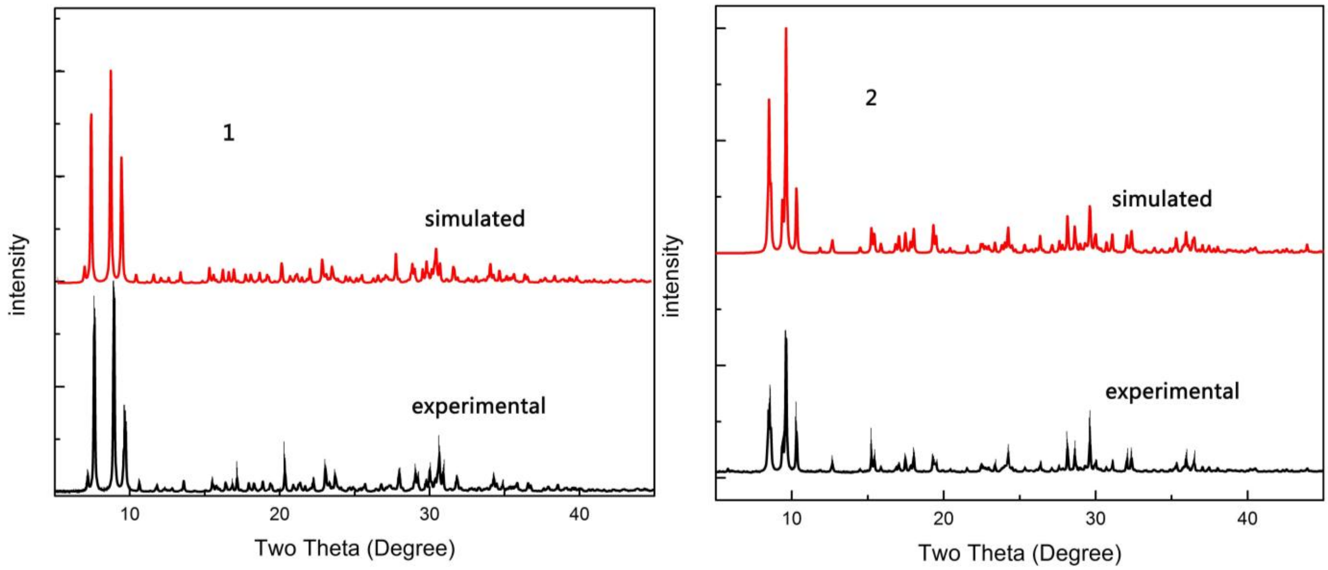

Figure S7. PXRD patterns of solids **1**-**2**, showing the bulk product are in good agreement with the calculated patterns based on the results from single-crystal X-ray diffraction.

The diffraction peaks on both patterns of **1**/**2** corresponded well in position, indicating the phase purity. The difference in reflection intensities between the simulated and experimental patterns was due to the variation in preferred orientation of the powder sample during collection of the experimental XRD data.